Hot Rolling Process Simulation: Application to UIC-60 Rail Rolling

Armindo Guerrero*[,1], Javier Belzunce[2], Covadonga Betegón[3], Julio Jorge[1,*] and Francisco J. Vigil[1,*]

[1]Fundación ITMA, PEPA, C/ Calafates Nº 11, 33417 Avilés (Asturias) Spain, [2]Department of Material Science and Metallurgical Engineering, University of Oviedo, 33203 Gijón (Asturias) Spain, [3]Department of Construction and Fabrication Engineering, University of Oviedo, 33203 Gijón (Asturias) Spain

Received: June 8, 2009; Accepted: July 30, 2009; Revised: November 27, 2009

Abstract: The aim of this paper is to present the developed procedure for the simulation of the hot rolling process also referring to some patents. Rolling is a 3D process but using the generalized plane strain method, the real 3D problem can be solved using 2D Finite Element Model (FEM), saving an important computing time. Thus, this procedure is really useful to give assistance in the roll design and to obtain the stock cross-section temperature distribution in the whole rolling process. On the other hand, it is also presented the thermo-mechanical characterization of the R260 quality steel, 0.7% C pearlitic steel, commonly used in rail rolling. Finally, the procedure is applied to simulate the UIC-60 rail hot rolling. A good agreement between FEM results and the sample shapes was obtained in the ArcelorMittal, S.A. rail mill facility in Asturias (Spain).

Keywords: Hot rolling process simulation, rail rolling & finite element analysis.

1. INTRODUCTION

In metal forming, a simple geometry, bloom or billet, is plastically deformed between tools to obtain the desired geometry [1-15].

Hot rolling is one of the main metal forming processes. In this process, the stock (bloom), after reheating, passes through three rolling stands, each one with different number of grooves. In each pass, the stock cross-section is reshaped and reduced. After the final pass, the stock comes off the roll mill with the desired rail shape [1, 8, 9, 12-14, 16].

This work corresponds to the procedure development for the simulation of the hot rolling process and its application to the hot rolling of UIC-60 rail. The full rolling process of this rail consists of seven shape passes in different grooves, only one pass in each groove (three in the roughing stand, three in the intermediate stand and the last one in the finishing stand).

The aim of this work is to validate the developed model in order to use it in two different ways:

- Give assistance to roll design; and
- Obtaining the stock cross-section temperature distribution during the whole rolling process.

The simulation was carried out using the finite element method, with the ANSYS code [17], applying the generalized plane strain procedure for modeling the 3D problem using a 2D formulation, reducing the computational cost time, in order to make the procedure really useful for rail producers.

The thermo-mechanical properties of the steel were obtained by means of an extensive testing program and the adjustment of the Peirce model was performed and verified to take into account the viscoplastic behavior of the steel.

Finally, the simulation results were compared with sample geometries of the rolling rail after every pass given into all the different shape grooves. These samples were obtained in the ArcelorMittal, S.A. rail mill facility in Asturias (Spain), and the agreement between both simulation and sample geometry was evaluated.

2. EXPERIMENTAL TESTING

The continuous advances in computer hardware and simulation codes allow the simulation of complex plastic forming processes. However, the accuracy of these simulations strongly depends on the reliability of the material data, being the true stress - true strain curves the most important data, which must cover completely the thermal and strain rate range of the process.

2.1. Material

R260 quality, 0.7% C pearlitic steel, supplied by ArcelorMittal, S.A. was used to obtain the specimens for testing. Table **1** presents the chemical composition of this steel according to the standard [18].

2.2. Mechanical Characterization

With the aim of performing a proper material characterization to obtain the viscoplastic behavior of the steel, the steps presented by Poursina *et al*. [19] were followed and tests were carried out at 800, 950, 1100 and 1300 ºC at different strain rates, 0.001, 0.1, 1.0 and 10 s^{-1}.

Cylindrical specimens of 5 mm diameter and 10 mm lenght were tested with a DIL 805A/D Bähr dilatometer,

*Address correspondence to these authors at the Fundación ITMA. PEPA, C/ Calafates Nº 11, 33417 Avilés (Asturias) Spain; Tel: +34 985 129 120; Fax: +34 985 129 008; E-mails: m.armindo@itma.es; j.jorge@itma.es; f.vigil@itma.es

1874-477X/10 $100.00+.00

Table 1. R260 Quality. Chemical Composition

% By Mass				10^{-4} % ppm Max by Mass
C	**Si**	**Mn**	**P**	**O**
0.60 - 0.82	0.13 - 0.60	0.65 - 1.25	0.030	20
Cr max	Al max	V max	N max	H
0.15	0.004	0.030	0.010	2.5
Mo max	Ni max	Cu max	Sn max	Sb max
0.02	0.10	0.15	0.030	0.020
Ti max	Nb max	Cu & 10 Sn max	Others Cr + Mo + Ni + Cu + V	
0.025	0.01	0.35	0.35	

which includes a deformation head. Each specimen was firstly heated up to the testing temperature and kept at this temperature so that the process remains isotherm. Then, the specimen was compressed until the specimen lenght was reduced to the half, true strain, $\varepsilon = \ln (L_F/L_0)$, = 0.693. Finally, the specimen was cooled down to room temperature. During the test, all the thermo-mechanical variables, such us stress, load, strain, strain rate, temperature, time and lenght change were automatically recorded by the dilatometer and later they were used to simulate the test by means of finite element method.

As an example, Fig. (**1**) shows the results of the tests carried out at 800 ºC.

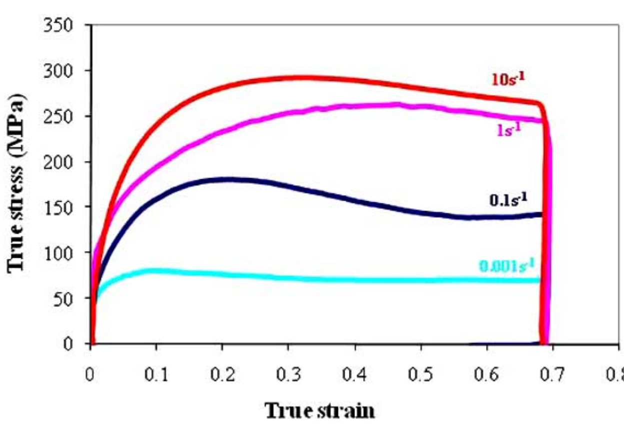

Fig. (1). True stress - true strain compression curves at 800ºC.

2.2.1. Viscoplastic Behavior of Material

Once the testing program was concluded, all the true stress - true strain curves were processed to implement the viscoplastic behavior of the material in the finite element code.

The ANSYS code allows to introduce the strain rate effect in the material model to simulate the time-dependent response of materials. In fact, two material options are available, the Perzyna (1) and the Peirce (2) models, and in contrast to other rate-dependent material options such as Anand's model, these models also include a yield surface. The plasticity and thus the strain rate hardening effect are active only after plastic yielding. So these models must be used in combination with the bilinear/multilinear or nonlinear isotropic hardening material options to simulate viscoplasticity [20].

$$\sigma = \left[1 + \left(\frac{\dot{\varepsilon}^{pl}}{\gamma}\right)^m\right]\sigma_0 \qquad (1)$$

$$\sigma = \left[1 + \left(\frac{\dot{\varepsilon}^{pl}}{\gamma}\right)\right]^m \sigma_0 \qquad (2)$$

Where: σ = material yield stress

$\dot{\varepsilon}^{pl}$ = equivalent plastic strain rate

m = strain rate hardening parameter

γ = material viscosity parameter

σ_0 = static yield stress of material

Both models refer to the steady state (ε_s), which is attained after some applied initial strain, once the full material recrystallization has taken place, see Fig. (**2**).

Thus, the stress values used in the adjustment were always the stress at the steady state, where it is possible to assume a complete recrystallization of the previously deformed microstructure. Figure **3** presents this simplification applied to the test curves obtained at 800ºC.

In this case, both models were checked and afterwards the Peirce model in combination with a multilinear isotropic hardening material option was considered the most appropriate. Table **2** summarizes the calculated values of the Peirce parameters (**σ_0**, **m** and **γ**).

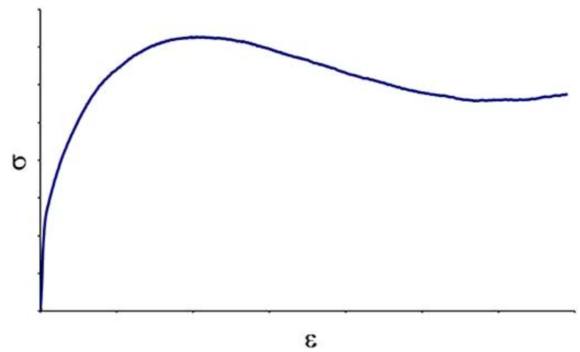

Fig. (2). Stress - strain curve. Evidence of strain hardening and recrystallization up to the attainment of the steady state.

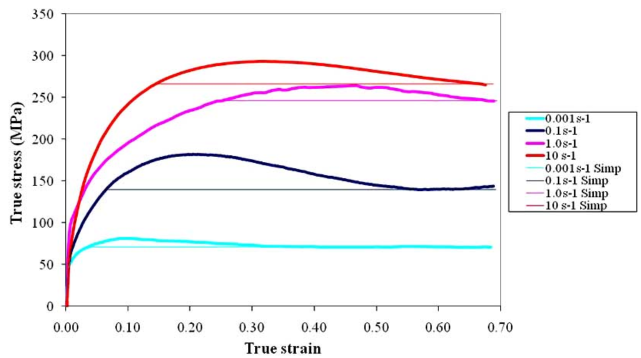

Fig. (3). Test curves simplification (800ºC).

Table 2. Adjustment Parameters

Temperature (ºC)	800	950	1110	1300
s	70.87	38.04	20.24	2.69
m	0.1404	0.1802	0.2158	0.2555
g	8.141E-04	2.539E-03	4.000E-03	5.079E-05

2.2.2. Viscoplastic Material Implementation into the ANSYS Code

In order to verify the material model implemented in ANSYS, in spite of the already mentioned simplification, the compression tests were simulated at every temperature and strain rate by means of an axisymmetryc finite element specimen model. The comparison of the applied load versus clamp displacement between simulations and tests showed in Fig. (**4**), gives an idea about the adjustment accurancy.

2.3. Thermal Characterization

The simulation of a hot rolling process means to carry out as many thermal transient analyses as the number of the different groove shapes has the process. The specific heat and the thermal conductivity of the steel are very important physical property needed in this simulation.

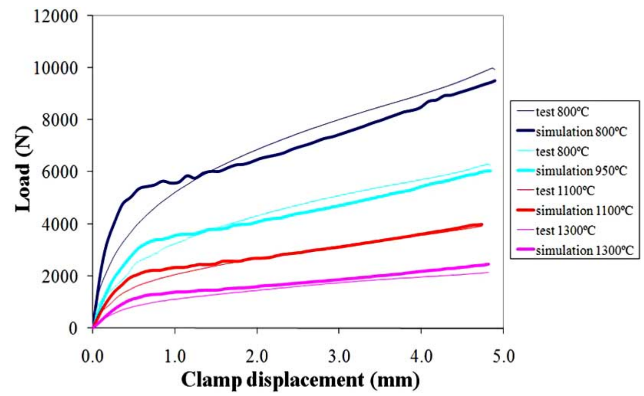

Fig. (4). Simulation vs. tests (800ºC, $10s^{-1}$).

A cylindrical specimen of 5 mm diameter and 1 mm height (aprox. 147.5 mg weight) was tested in a PG 409 P LUXX Netzsch thermobalace by means of applying a thermal cycle up to 1300ºC (10 ºC/min). Figure **5** shows the evolution of the specific heat with the temperature.

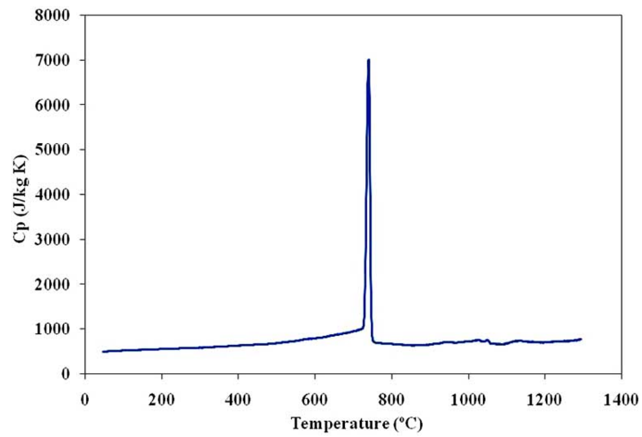

Fig. (5). Specific heat (J/kg K).

The steel thermal conductivity was obtained from the literature [21], AISI 1078 steel (G10780), with a similar chemical composition to R260 quality. Table **3** presents the values used in the analyses.

Table 3. Thermal Conductivity (W/m K)

Temperature (ºC)	0	100	200	300	400	500
K (W/m K)	48.7	48.2	45.2	41.4	38.1	35.2
Temperature (ºC)	600	700	800	900	1000	1200
K (W/m K)	32.7	30.1	24.3	25.6	26.8	30.1

2.4. Measurement Performed in the Rail Mill

To simulate the UIC-60 rail rolling and compare the simulation to the reality, it was necessary to carry out an extensive program of measurements. All the measurements were taken in the ArcelorMittal, S.A. rail mill facility.

The time between the rail entrance into the different grooves was measured and taken into account in the simulation of the hot rolling process.

On the other hand, to verify the results of temperature obtained by means of the simulation the stock temperature on the external surface at the entrance into each groove in the whole rolling process was recorded. Temperature measurements were obtained by means of thermography, using the infrared camera ThermaCAM™ P65.

Previously the emissivity (ε) of the camera was adjusted carrying out some laboratory tests, and the emissivity was set as follows:

- ε = 0.91 in the roughing and intermediate stand.
- ε = 0.93 in the finishing stand.

3. FINITE ELEMENT MODEL

Rail hot rolling is a multi-pass process where the initial rectangular cross-section geometry of a bloom is transformed into the desired rail shape by means of a sequential forming performed by successive passes between pairs of shaped rolls (grooves).

Thus, the simulation of the whole process can be considered as the simulation of as many stages, almost independent, as the number of grooves used in the rail mill for rolling the considered rail. The only differences in the simulation of two any stages of the whole process are the initial cross-section and the temperature distribution at the beginning of the stage.

3.1. Analysis Procedure

The whole multi-pass process simulation was carried out by means of the procedure which is described herein and represented graphically in Fig. (**6**).

3.1.1. Transient Thermal Analyses

Simulation of any intermediate stage "i" starts with a transient thermal analysis, which simulated the heat loss of the stock from the exit of groove "i-1" up to the entrance into groove "i" and also the one due to fluid cooling during the rolling in groove "i-1".

The finite element model built for these analyses use the PLANE55 finite element, from the ANSYS library [17].

In these analyses, the main load was the initial temperature, constant and equal to 1260ºC on the whole cross-section at the beginning of the process. For the rest of the stages, since the structural simulation was considered isothermal, the initial temperature for the analysis of groove "i" was just the obtained at the end of the analysis performed in groove "i-1".

On the other hand, convective heat transfer boundary conditions plus radiation to the ambient environment were taken into account. The parameter which governs the convection, the film coefficient, was adjusted in order to match the temperature profile on the external surface of the stock, according to the measurement carried out in the rail mill.

The time length of this analysis was the time between the entrance into two consecutive grooves, measured in the ArcelorMittal S.A. rail mill facility.

3.1.2. Structural Analyses

First of all, the structural analyses in the process simulation do not consider heat losses, i.e., the forming operation itself is considered as isothermal.

The stock cross-section geometry used to perform the structural analysis of the "i" stage was the same than the one used in the previous thermal analysis, as well as the mesh, but changing the finite element type: thermal to structural, from PLANE55 to PLANE182 [17]. This last element presents as option some of the special features (generalized plane strain, viscoplasticity, large strain, initial stress import, manual rezoning possibility) needed to perform the rolling process simulation.

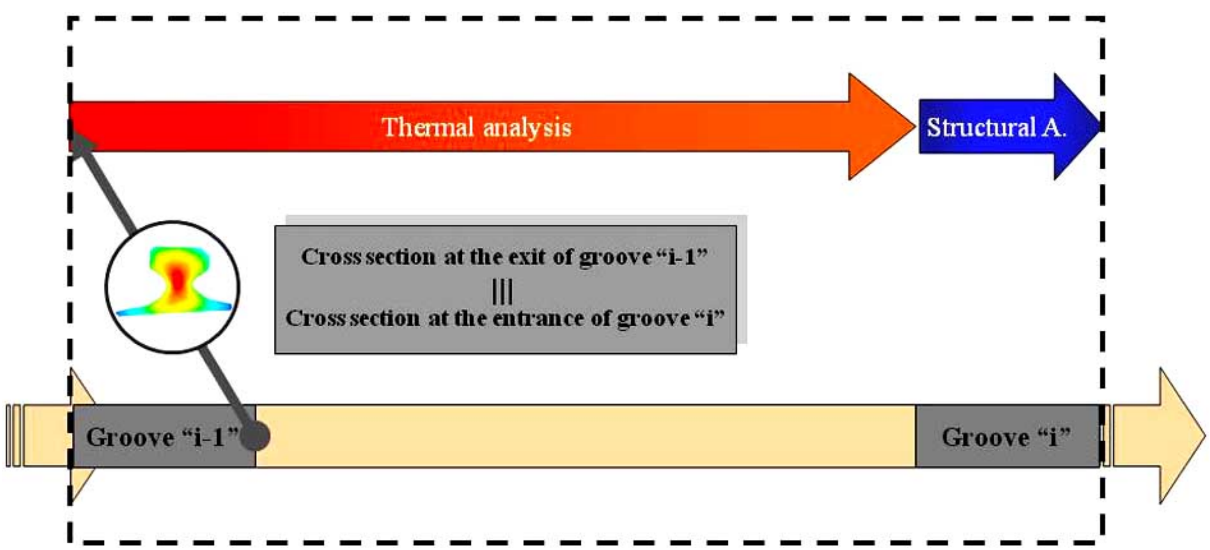

Fig. (6). General procedure scheme of rolling analysis.

Besides, with the stock cross-section, the shapes of the roll grooves have to be imported from external IGES files and positioned just in contact with the stock cross-section mesh. Thus, the closure of the rolls will simulate the rolling operation itself.

The rolls were considered as non-deformable rigid bodies and the heat transfer between them and the stock cross-section was not taken into account. Friction between stock and rolls was modelled using the Coulomb friction law with a friction coefficient, $\mu = 0.2$.

In the course of these analyses, due to the viscoplastic material model used in the simulation, it is very important to take into account the real time between the different forming operations. So the time for each analysis was estimated according to the rolled length and the velocity of the rolls see Fig. (**7**).

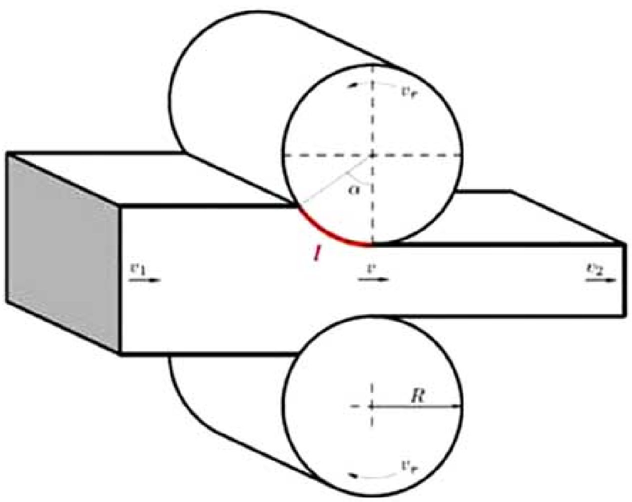

Fig. (7). Material & rolls contact in flat rolling.

During these analyses, due to the huge applied deformation, the mesh distortion could not be acceptable, so that in such case, the mesh was repaired as many times as it was necessary to keep the quality of the grid until the end of the simulation.

4. RESULTS

The evolution of the UIC-60 rail rolling can be seen in Figs. (**8**) to (**15**). Each of these figures consists of three pictures:

- The sample photograph, which shows the geometry obtained in the ArcelorMittal S.A. rail mill facility at the exit of each groove.
- The result of the simulation at the end of the same groove, stock cross-section with the prediction of temperature distribution.
- The overlap of both images with the second one in semi-transparent format in order to analyze the shape prediction accurancy.

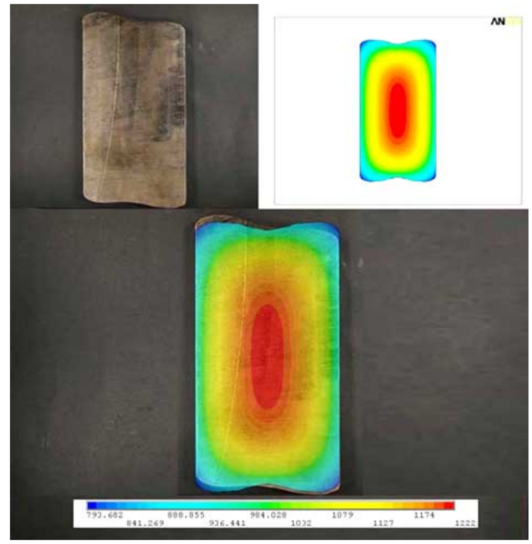

Fig. (8). Comparison at the entrance of groove # 3.

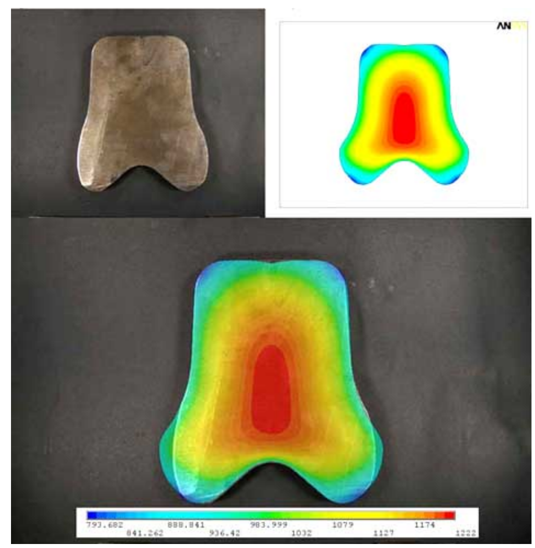

Fig. (9). Comparison at the exit of groove # 3.

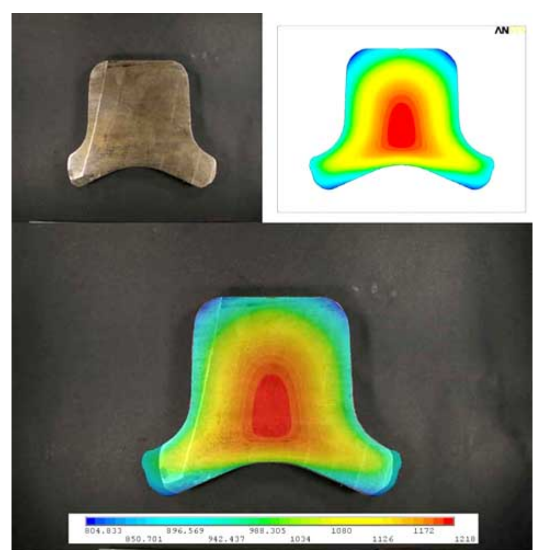

Fig. (10). Comparison at the exit of groove # 4.

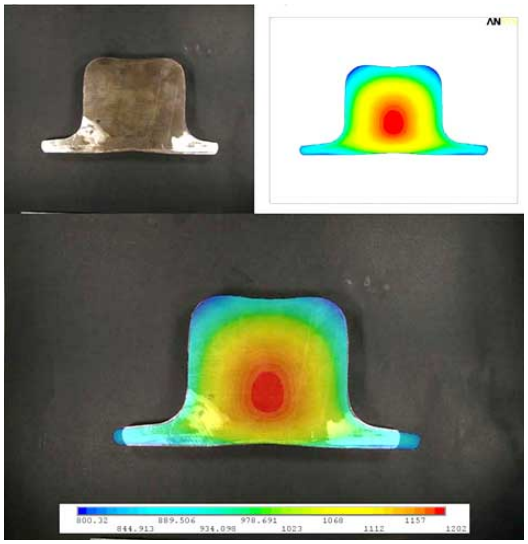

Fig. (11). Comparison at the exit of groove # 5.

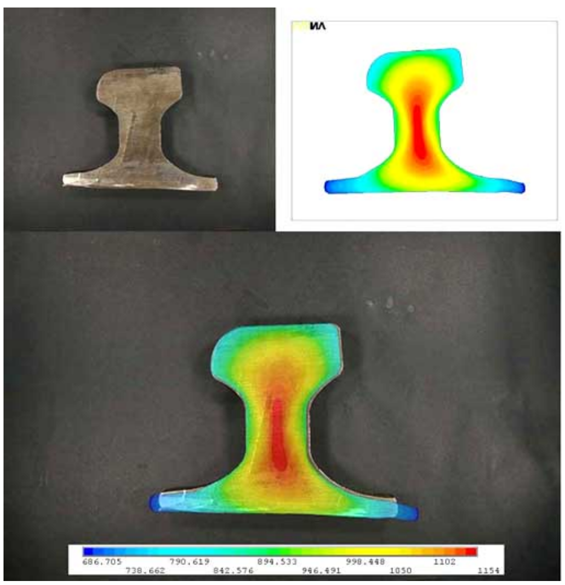

Fig. (12). Comparison at the exit of groove # 8.

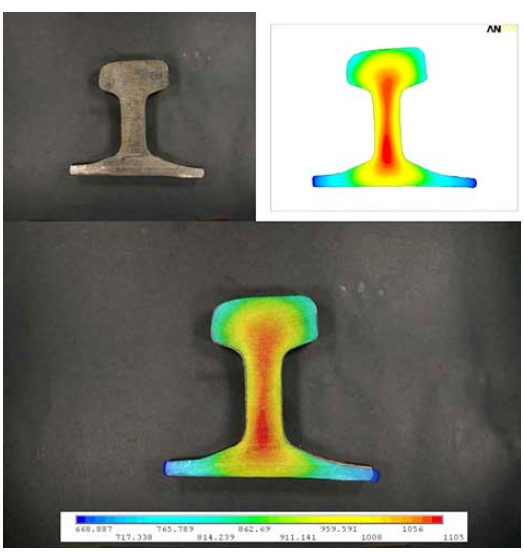

Fig. (13). Comparison at the exit of groove # 9.

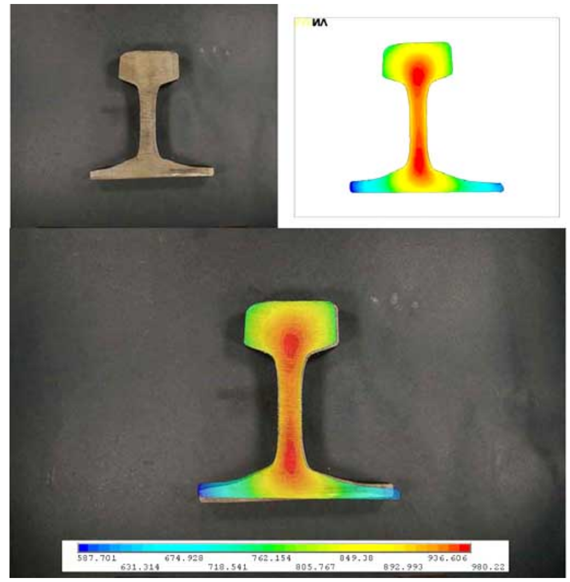

Fig. (14). Comparison at the exit of groove # 10.

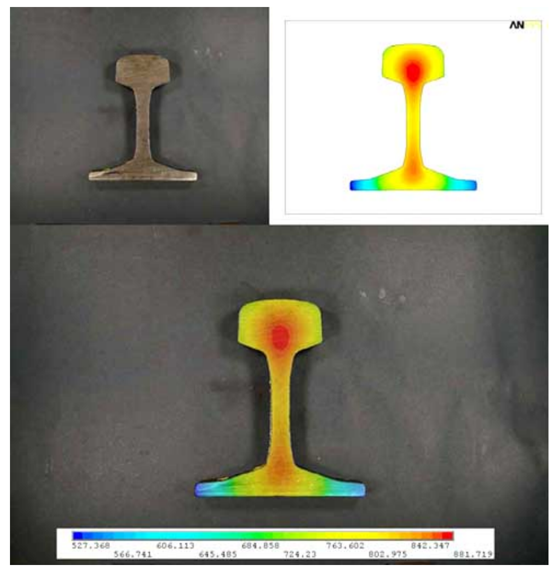

Fig. (15). Comparison at the exit of groove # 11.

5. CONCLUSION

A good shape agreement between the samples obtained in the rail mill facility and the predictions made with the finite element analyses was obtained, so that the described procedure can be considered as a powerful tool to help experts to roll design. Thus, the number of trials needed to carry out the rolling of a new shape rail would be decreased and also rolling productivity could be increased, removing non-efficient grooves.

On the other hand, the film coefficients were adjusted so that the temperature profile on the external surface of the stock, at the entrance into each groove and at the end of the process matched the temperature measurement on the rail mill. Once this adjustment was done, a good prediction of the temperature distribution in the rail cross-section is available at the end of the process.

6. CURRENT & FUTURE DEVELOPMENTS

A numerical study on the thermo-structural behaviour during the hot rolling process simulation of UIC60 rails has been presented.

This work could be very useful for further processes, e.g. head hardening of the rail, in which the temperature distribution after the roll forming process would be an input of the head hardening process, helping to design the insulation and/or induction coils necessary to achieve the desired final microstructure of the rail head.

Furthermore, this hot rolling process simulation could also be used as an input for the rail straightening process design and optimization.

ACKNOWLEDGEMENTS

This research has been supported by ArcelorMittal, S.A.

CONFLICT OF INTEREST

The authors have no conflict of interest.

REFERENCES

[1] Ueda, M., Fujita, K., Matsushita, K., Yamamoto, T., Satoh, T.: EP1730317 **(2006)**.
[2] Keyzer, P.L., Kiefer, B.V., Shore, T.M.: CA2420016C **(2002)**.
[3] Shore, T.M., Keyzer, P.L., Kiefer, B.V., Keyzer, P.L.: EP1315585 **(2003)**.
[4] Shore, T.M., Keyzer, P.L., Kiefer, B.V.: US6546777 **(2003)**.
[5] Shore, T.M., Keyzer, P.L., Kiefer, B.V.: US20020046590 **(2002)**.
[6] Engel, G., Mauk, P.J., Nowak, H.-J., Svejkovsky, U.: EP0818250B1 **(2002)**.
[7] Keyzer, P.L., Kiefer, B.V., Shore, T.M.: CA2420016AA **(2002)**.
[8] Kishikawa, K., Nishino, T., Nagasoe, S.: US4503699 **(1985)**.
[9] Kishikawa, K., Nishino, T.: US4503700 **(1985)**.
[10] Hioki, T., Shimizu, S., Hokimoto, T.: US5896770 **(1999)**.
[11] Engel, G., Mauk, P.J., Nowak, H.-J., Svejkovsky, U.: EP0818250A3 **(1999)**.
[12] Kovacs, D.C.: US4393680 **(1983)**.
[13] Kozono, H., Higashinaka, H.: US4344310 **(1982)**.
[14] Ishibashi, Y., Kishikawa, K.: US3657912 **(1972)**.
[15] Kobayashi S, Oh S-I, Altan T. Metal forming and the finite element method (Oxford Series on Advanced Manufacturing). Oxford University Press: USA 1989.
[16] Riljak S. Numerical simulation of shape rolling. PhD Dissertation, Royal Institute of Technology, Stockholm, Sweden 2006: SE-100 44.
[17] ANSYS Engineering Analysis System. Rev. 11.1, ANSYS Inc. Canonsburg PA, USA.
[18] EN 13674-1. Railway applications. Track. Rail. Vignole railway rails 46 kg/m and above. October 2003.
[19] Poursina M, Ebrahimi H, Parvizian J. Flow stress behaviour of two stainless steels: An experimental-numerical investigation. J Mater Process Tech 2008; 199: 287-294.
[20] Theory Section 4.2. Rate Depend Plasticity. ANSYS Help, 2005.
[21] Cverna F. Thermal properties of metals. ASM International, Ohio: USA 2002.